

Weierstraß-Institut
für Angewandte Analysis und Stochastik
Leibniz-Institut im Forschungsverbund Berlin e. V.

Preprint

ISSN 2198-5855

**Higher order continuous Galerkin–Petrov time stepping
schemes for transient convection-diffusion-reaction
equations**

Naveed Ahmed¹, Gunar Matthies²

submitted: August 7, 2014

¹ Weierstrass Institute
Mohrenstr. 39
10117 Berlin
Germany
email: Naveed.Ahmed@wias-berlin.de

² Universität Kassel, Institut für Mathematik
Heinrich-Plett-Str. 40
34132 Kassel
Germany
email: matthies@mathematik.uni-kassel.de

No. 1990
Berlin 2014



2010 *Mathematics Subject Classification.* 65M12, 65M15, 65M60.

Key words and phrases. transient convection-diffusion-reaction problem, local projection stabilization, continuous Galerkin–Petrov method, discontinuous Galerkin method.

This research work was partially supported by the German research foundation (DFG) under the grant MA 4713/2-1.

Edited by
Weierstraß-Institut für Angewandte Analysis und Stochastik (WIAS)
Leibniz-Institut im Forschungsverbund Berlin e. V.
Mohrenstraße 39
10117 Berlin
Germany

Fax: +49 30 20372-303
E-Mail: preprint@wias-berlin.de
World Wide Web: <http://www.wias-berlin.de/>

Abstract. We present the analysis for the higher order continuous Galerkin-Petrov (cGP) time discretization schemes in combination with the one-level local projection stabilization in space applied to time-dependent convection-diffusion-reaction problems. Optimal a-priori error estimates will be proved. Numerical studies support the theoretical results. Furthermore, a numerical comparison between continuous Galerkin-Petrov and discontinuous Galerkin time discretization schemes will be given.

INTRODUCTION

In recent years many numerical methods have been developed for the numerical solution of time-dependent convection-diffusion-reaction equations. Some of the most effective and popular algorithms for treating time-dependent problems can be defined through a process in which the spatial and temporal discretization are separated. A common approach is to first apply the Galerkin method in space to reduce the time-dependent partial differential equation into a system of ordinary differential equations. A suitable time discretization method is then applied to solve it. An alternative to this approach is a coupled space-time formulation which results in a system where all degrees inside the space-time cylinder are coupled. Hence, a $(d + 1)$ -dimensional problem is discretized for a spatial domain with d dimensions. We will separate in this paper the discretizations in space and time.

The application of standard finite element methods to convection-dominated problems leads to spurious oscillations which spread over the whole spatial domain unless the discretization parameter in space is unpractically small.

To overcome the instability while ensuring high accuracy, several stabilized techniques were proposed in the literature. One of the popular remedies is the streamline-upwind Petrov-Galerkin (SUPG) method which was introduced by Hughes and Brooks [15]. The SUPG method was originally proposed for steady state problems

and has been extended to transient problem, see [8, 22]. Standard energy arguments applied to the fully discrete problem yield error estimates under conditions which couple the choice of the stabilization parameters to the length of the time step. In particular, the SUPG stabilization vanishes in the time-continuous limit. This behavior is caused by the time derivative appearing in the stabilization terms of the SUPG method to guarantee the strong consistency. The appearing non-symmetric term is difficult to handle in the numerical analysis. Using a different analysis for the case of time independent coefficients on uniform grids, optimal error estimates with the standard choice of the stabilization parameter independent of the time step length have been proved and confirmed by numerical experiments, see [22].

Comparisons of the SUPG method with other stabilization techniques can be found in [11, 26]. The stability of consistent stabilization methods for convection-diffusion and flow problems in the small time step limit has been investigated in [6, 14].

A stabilization technique which became very popular during last decade is the local projection stabilization (LPS) scheme [5, 7, 28]. The local projection method provides additional control on the fluctuations of the gradient or parts of its. Although, the method is weakly consistent only, the consistency error can be bounded such that the optimal order of convergence is maintained. Originally proposed for the Stokes problem [4], the local projection method was extended successfully to transport problems [5], Oseen problems [7, 28] and convection-diffusion-reaction problems [29]. In contrast to the SUPG method, neither time derivatives nor second order spatial derivatives have to be assembled for the stabilization term of LPS. Furthermore, no coupling conditions of stabilization parameters to the length of the time step arise.

Using stabilization techniques in space leads to a dramatic decrease of the oscillations which appear now only close to boundary and interior layers. Moreover, the amplitudes are much smaller. To remove the remaining oscillations, techniques for shock or discontinuity capturing can be applied. Numerical and analytical results are given for instance in [18–20].

Accurate numerical solutions of time-dependent problems require higher order methods both in space and time. In this paper, we will apply higher order variational type time discretization schemes. In particular, we will use continuous Galerkin-Petrov (cGP) and discontinuous Galerkin (dG) time stepping schemes. The cGP methods are a class of finite element methods using discrete solution spaces in time which consist of continuous piece-wise polynomials of degree less than or equal to k and test spaces which are built by discontinuous polynomials of degree up to order $k - 1$. In dG methods, both solution and test spaces are constructed by the discontinuous polynomials of degree less than or equal to k . Since the test functions in time are for both considered temporal discretizations allowed to be discontinuous at the discrete time points, the solution of cGP and dG schemes can be calculated by a time marching process.

The dG methods were first introduced by Reed and Hill [30] for neutron transport problems. The use of continuous and discontinuous finite element methods to discretize time-dependent problems has been analyzed for ordinary and partial differential equations by several authors. The time discretization by discontinuous Galerkin methods was introduced and analyzed in [12] for the numerical solution of ordinary differential equations and is combined with continuous finite element methods in space for parabolic problem in [13, 33, 34].

The combination of LPS methods in space and dG methods in time has been analyzed for transient convection-diffusion-reaction problems in [2]. The continuous Galerkin method in time for the heat equation has been studied by Aziz and Monk in [3]. They have proved optimal error estimates as well as super-convergence results at the endpoints of the discrete time intervals. Schieweck [32] has investigated the cGP-method for linear ordinary differential equations in an abstract Hilbert-space setting and for nonlinear systems of ordinary differential equations in d space dimensions. He has proved A-stability and optimal error estimates of the associated cGP-method. Moreover, it was shown that this discretization method has an energy decreasing property for the gradient flow equation of an energy functional. Numerical comparisons of dG and cGP methods as time discretization of heat equations and transient Stokes problems are presented in [16, 17]. A family of finite element methods for the numerical solution of nonlinear systems of ordinary differential equations was recently given in [27]. Furthermore, it was shown there that the new methods can be interpreted as pure collocation and

pure variational methods with special numerical integration. In [27], simple post-processing algorithms were presented which allow to increase the obtained accuracy in time by one order in time-integrated norms.

The goal of the present paper is to combine the local projection stabilization in space with continuous Galerkin-Petrov discretizations in time. We will give a stability result and error estimates for the fully discrete scheme. Furthermore, a numerical comparison of cGP and dG time discretization schemes combined with LPS in space will be given.

This paper is organized as follows: In Section 1, a weak formulation of the time-dependent convection-diffusion-reaction equation and some basic notation are given. The semi-discretization in space and the local projection stabilization method are introduced in Section 2. Section 3 presents the fully discrete problem with a continuous Galerkin-Petrov time discretization and its error analysis. Finally, numerical results which confirm the theoretical prediction will be given in Section 4. Furthermore, a comparison to discontinuous Galerkin time discretization schemes will be presented.

1. MODEL PROBLEM

Let Ω be a polygonal or polyhedral domain in \mathbb{R}^d , $d = 2, 3$, with Lipschitz boundary $\partial\Omega$. We consider the following time-dependent convection-diffusion-reaction equation:

Find $u : \Omega \times [0, T] \rightarrow \mathbb{R}$ such that

$$\begin{cases} u' - \varepsilon \Delta u + \mathbf{b} \cdot \nabla u + \sigma u = f & \text{in } \Omega \times (0, T), \\ u = 0 & \text{on } \partial\Omega \times (0, T), \\ u(\cdot, 0) = u_0 & \text{in } \Omega \end{cases} \quad (1)$$

with a small positive constant $0 < \varepsilon \ll 1$, $\mathbf{b}(x)$ and $\sigma(x)$ are given function, u_0 the initial data, and $T > 0$ a given final time. We assume that \mathbf{b} and σ are time-independent whereas f may depend on time t . Furthermore, let the data \mathbf{b} , σ , u_0 , and f be sufficiently smooth in Ω and $\Omega \times (0, T)$, respectively. We assume in the following that there exists a positive constant σ_0 such that

$$\sigma(x) - \frac{1}{2} \operatorname{div} \mathbf{b}(x) \geq \sigma_0 > 0 \quad \text{in } \Omega. \quad (2)$$

Note that the assumption (2) is no restriction for time-dependent convection-diffusion-reaction problems of type (1). Indeed, if condition (2) is not fulfilled we consider the problem

Find $v : \Omega \times [0, T] \rightarrow \mathbb{R}$ such that

$$\begin{cases} v' - \varepsilon \Delta v + \mathbf{b} \cdot \nabla v + (\sigma + M)v = e^{-Mt} f & \text{in } \Omega \times (0, T), \\ v = 0 & \text{on } \partial\Omega \times (0, T), \\ v(\cdot, 0) = u_0 & \text{in } \Omega \end{cases}$$

for the function v defined by

$$v(x, t) := e^{-Mt} u(x, t).$$

If M is chosen sufficiently large then condition (2) is fulfilled for the modified problem for v .

Throughout this paper, standard notation and conventions will be used. For a measurable set $G \subset \mathbb{R}^d$, the inner product in $L^2(G)$ and $L^2(G)^d$ will be denoted by $(\cdot, \cdot)_G$. The norm and semi-norm in $W^{m,p}(G)$ are given by $\|\cdot\|_{m,p,G}$ and $|\cdot|_{m,p,G}$, respectively. In the case $p = 2$, we write $H^m(G)$, $\|\cdot\|_{m,G}$, and $|\cdot|_{m,G}$ instead of $W^{m,2}(G)$, $\|\cdot\|_{m,2,G}$, and $|\cdot|_{m,2,G}$. If $G = \Omega$, the index G in inner products, norms, and semi-norms will be omitted. The subspace of functions from $H^1(\Omega)$ having zero boundary trace is denoted by $H_0^1(\Omega)$.

We will write shortly $\alpha \sim \beta$ if there exist positive constants C_1 and C_2 such that $\alpha \leq C_1\beta$ and $\beta \leq C_2\alpha$ hold true.

We consider also some Bochner spaces. Let W be a Banach space with norm $\|\cdot\|_W$ and $I := [0, T]$. We define

$$\begin{aligned} C(I; W) &:= \{v : I \rightarrow W, \quad v \text{ continuous}\}, \\ L^2(I; W) &:= \left\{ v : I \rightarrow W, \quad \int_0^T \|v(t)\|_W^2 dt < \infty \right\}, \\ H^m(I; W) &:= \left\{ v \in L^2(I; W) : \frac{\partial^j v}{\partial t^j} \in L^2(I; W), \quad 1 \leq j \leq m \right\}, \end{aligned}$$

where the derivatives $\partial^j v / \partial t^j$, $j = 1, \dots, m$, are understood in the sense of distributions on I . We use in the following the short notation $Y(W) := Y(I; W)$. The norms in the above defined spaces are given by

$$\|v\|_{C(W)} := \sup_{t \in I} \|v(t)\|_W, \quad \|v\|_{L^2(W)} := \left(\int_0^T \|v(t)\|_W^2 dt \right)^{1/2}, \quad \|v\|_{H^m(W)} := \left(\sum_{j=0}^m \left\| \frac{\partial^j v}{\partial t^j} \right\|_{L^2(W)}^2 \right)^{1/2}.$$

Let us introduce the space $V := H_0^1(\Omega)$, its dual space $V' := H^{-1}(\Omega)$, and $\langle \cdot, \cdot \rangle$ for the duality product between these two spaces.

A function u is a weak solution of problem (1), if

$$u \in X := \{u \in L^2(V) : u' \in L^2(V')\} \quad (3)$$

with

$$\langle u'(t), v \rangle + a(u(t), v) = \langle f(t), v \rangle \quad \forall v \in V \quad (4)$$

for almost all $t \in I$ and

$$u(0) = u_0, \quad (5)$$

where the bilinear form a is given by

$$a(u, v) := \varepsilon(\nabla u, \nabla v) + (\mathbf{b} \cdot \nabla u, v) + (\sigma u, v).$$

Note that the definition of X in (3) implies the continuity of u as a mapping $I \rightarrow L^2(\Omega)$ such that the initial condition (5) is well-defined.

Integrating (4) over $[0, T]$, we obtain the problem:

Find $u \in X$ with $u(0) = u_0$ and

$$\int_0^T \langle u'(t), v(t) \rangle + a(u(t), v(t)) dt = \int_0^T \langle f(t), v(t) \rangle dt \quad \forall v \in L^2(V). \quad (6)$$

In the following, we shall denote by φ' , φ'' , and $\varphi^{(k)}$ the first, second, and k -th order time derivative of a function φ which is sufficiently smooth in time.

For finite element discretizations of (6), let $\{\mathcal{T}_h\}$ denote a family of shape regular triangulations of Ω into open d -simplices, quadrilaterals, or hexahedra such that

$$\bar{\Omega} = \bigcup_{K \in \mathcal{T}_h} \bar{K}.$$

The diameter of $K \in \mathcal{T}_h$ will be denoted by h_K and the mesh size h is defined by $h := \max_{K \in \mathcal{T}_h} h_K$. Let V_h be a finite element space defined on \mathcal{T}_h such that the inverse inequality

$$\|\nabla v_h\|_{0,K} \leq c_{\text{inv}} h_K^{-1} \|v_h\|_{1,K}$$

holds for all $K \in \mathcal{T}_h$ and all $v_h \in V_h$ where the constant c_{inv} is independent of K and h . We set $X_h := \mathbf{H}^1(V_h)$. Let $u_{0,h} \in V_h$ denote a suitable approximation of the initial condition u_0 . Later on, $u_{0,h}$ will be specified.

The standard Galerkin method applied to problem (6) consists in

Find $u_h \in X_h$ such that $u_h(0) = u_{0,h}$ and

$$\int_0^T (u_h'(t), v_h(t)) + a(u_h(t), v_h(t)) dt = \int_0^T (f(t), v_h(t)) dt \quad \forall v_h \in L^2(V_h). \quad (7)$$

In the convection-dominant case $\varepsilon \ll 1$, it is well-known that the standard Galerkin method (7) applied to problem (1) is unstable and leads to solutions which are globally polluted by spurious oscillations unless the discretization parameter h is unpractically small.

2. SPATIAL STABILIZATION BY THE LPS METHOD

We concentrate on the one-level local projection stabilization method in which approximation space and projection space are defined on the same mesh. Let $D(K)$, $K \in \mathcal{T}_h$, be finite dimensional spaces and $\pi_K : L^2(K) \rightarrow D(K)$ the local L^2 -projection into $D(K)$. The local fluctuation operator $\kappa_K : L^2(K) \rightarrow L^2(K)$ is given by $\kappa_K v := v - \pi_K v$. The stabilization term S_h is defined by

$$S_h(u_h, v_h) := \sum_{K \in \mathcal{T}_h} \mu_K (\kappa_K \nabla u_h, \kappa_K \nabla v_h)_K$$

where μ_K , $K \in \mathcal{T}_h$, are user chosen non-negative constants. The fluctuation operator is applied component-wise to vector-valued functions. The used local projection stabilization gives additional control on the fluctuation of the gradient. Note that one can replace the gradient ∇w_h by the derivative in streamline direction $\mathbf{b} \cdot \nabla w_h$ or (even better [24, 25]) by $\mathbf{b}_K \cdot \nabla w_h$ where \mathbf{b}_K is a piece-wise constant approximation of \mathbf{b} .

Stability and convergence properties of local projection methods are based on the following assumptions with respect to the approximation space V_h and the local projection spaces $D(K)$, $K \in \mathcal{T}_h$, see [28, 31].

Assumption 1. *There is an interpolation operator $j_h : \mathbf{H}^2(\Omega) \rightarrow V_h$ such that for all $K \in \mathcal{T}_h$ the standard error estimate*

$$\|v - j_h v\|_{0,K} + h_K |v - j_h v|_{1,K} \leq C h_K^l \|v\|_{l,K} \quad \forall v \in \mathbf{H}^l(K), \quad 2 \leq l \leq r+1, \quad (8)$$

and the additional orthogonality condition

$$(v - j_h v, q_h)_K = 0 \quad \forall v \in \mathbf{H}^2(\Omega), \quad \forall q_h \in D(K) \quad (9)$$

hold true.

Assumption 2. *The fluctuation operators κ_K , $K \in \mathcal{T}_h$, satisfy the following approximation property*

$$\|\kappa_K q\|_{0,K} \leq C h_K^l |q|_{l,K} \quad \forall q \in \mathbf{H}^l(K), \quad 0 \leq l \leq r. \quad (10)$$

Using the interpolation operator j_h , we will use $u_{0,h} = j_h u_0$ as discrete initial condition. Then, the stabilized semi-discrete problem for u_h reads:

Find $u_h \in X_h$ such that $u_h(0) = j_h u_0$ and

$$\int_0^T (u_h'(t), v_h(t)) + a_h(u_h(t), v_h(t)) dt = \int_0^T (f(t), v_h(t)) dt \quad \forall v_h \in L^2(V_h) \quad (11)$$

where the stabilized bilinear form a_h is given by

$$a_h(u_h, v_h) := a(u_h, v_h) + S_h(u_h, v_h).$$

Thanks to (2) we have

$$a_h(v_h, v_h) \geq \|v_h\|^2 \quad \forall v_h \in V_h, \quad (12)$$

i.e., the bilinear form a_h is coercive with respect to the mesh-dependent norm

$$\|v\| = \{\varepsilon|v|_1^2 + \sigma_0\|v\|_0^2 + S_h(v, v)\}^{1/2}. \quad (13)$$

3. TIME DISCRETIZATION

We discretize in this section problem (11) in time by using continuous Galerkin-Petrov methods and discontinuous Galerkin methods. To this end, we consider a partition $0 = t_0 < t_1 < \dots < t_N = T$ of the time interval I and set $I_n := (t_{n-1}, t_n]$, $\tau_n := t_n - t_{n-1}$, $n = 1, \dots, N$, and $\tau := \max_{1 \leq n \leq N} \tau_n$. For a given non-negative integer k , we define the spaces

$$\begin{aligned} X^k &:= \left\{ u \in C(I, V) : u|_{I_n} \in \mathbb{P}_k(I_n, V), \quad n = 1, \dots, N \right\}, \\ Y^k &:= \left\{ v \in L^2(I, V) : v|_{I_n} \in \mathbb{P}_k(I_n, V), \quad n = 1, \dots, N \right\} \end{aligned}$$

with values in V and the fully discrete spaces

$$\begin{aligned} X_h^k &:= \left\{ u \in C(I, V_h) : u|_{I_n} \in \mathbb{P}_k(I_n, V_h), \quad n = 1, \dots, N \right\}, \\ Y_h^k &:= \left\{ v \in L^2(I, V_h) : v|_{I_n} \in \mathbb{P}_k(I_n, V_h), \quad n = 1, \dots, N \right\} \end{aligned}$$

with values in V_h where

$$\begin{aligned} \mathbb{P}_k(I_n, V) &:= \left\{ u : I_n \rightarrow V : u(t) = \sum_{j=0}^k U^j t^j, \quad U^j \in V, \quad j = 0, \dots, k \right\}, \\ \mathbb{P}_k(I_n, V_h) &:= \left\{ u_h : I_n \rightarrow V_h : u_h(t) = \sum_{j=0}^k U_h^j t^j, \quad U_h^j \in V_h, \quad j = 0, \dots, k \right\} \end{aligned}$$

denote the spaces of V -valued and V_h -valued polynomials of order up to k in time, respectively. The functions in the spaces Y^k and Y_h^k are allowed to be discontinuous at the nodes t_n , $n = 1, \dots, N-1$. We define for

functions $v \in Y^k + Y_h^k$ by

$$v_n^- := \lim_{t \rightarrow t_n^-} v(t), \quad v_n^+ := \lim_{t \rightarrow t_n^+} v(t), \quad [v]_n := v_n^+ - v_n^-, \quad (14)$$

the left-sided value v_n^- , right-sided value v_n^+ , and the jump $[v]_n$.

3.1. The continuous Galerkin-Petrov (cGP) method

We describe in this section the combination of the continuous Galerkin-Petrov (cGP) time discretization scheme with the LPS finite element method in space to get a fully discrete version of (11).

Now, let us introduce the bilinear forms B , B_h and the linear form l as

$$B(u, v) := \int_0^T \left\{ (u'(t), v(t)) + a(u(t), v(t)) \right\} dt, \quad (15)$$

$$B_h(u, v) := \int_0^T \left\{ (u'(t), v(t)) + a_h(u(t), v(t)) \right\} dt, \quad (16)$$

$$l(v) := \int_0^T (f(t), v(t)) dt. \quad (17)$$

Then, the continuous and fully discrete problems read:

Find $u \in X$ such that $u(0) = u_0$ and

$$B(u, v) = l(v) \quad \forall v \in L^2(V). \quad (18)$$

Find $u_{h,\tau} \in X_h^k$ such that $u_{h,\tau}(0) = j_h u_0$ and

$$B_h(u_{h,\tau}, v_{h,\tau}) = l(v_{h,\tau}) \quad \forall v_{h,\tau} \in Y_h^{k-1}. \quad (19)$$

Since the test functions are allowed to be discontinuous at the discrete time points t_n , $n = 1, \dots, N-1$, we can choose test functions $v_{h,\tau} = v_h \varphi(t)$ with a time independent $v_h \in V_h$ and a scalar function $\varphi : I \rightarrow \mathbb{R}$ which is zero on $I \setminus I_n$ and a polynomial of degree less than or equal to $k-1$ on I_n . Then, the solution of the cGP(k)-method can be determined by successively solving one local problem on each time interval I_n .

Let us denote by $\pi_{k-1} : L^2(L^2) \rightarrow Y_h^{k-1}$ the L^2 -projection onto space of V_h -values functions which are allowed to be discontinuous at the discrete time points. Hence, we have

$$\pi_{k-1} w \in Y_h^{k-1}, \quad \int_{I_n} (w(t) - \pi_{k-1} w(t)) t^j dt = 0, \quad j = 0, \dots, k-1. \quad (20)$$

We consider the mesh-dependent norm

$$\|v\|_{\text{cGP}} = \left(\int_0^T \|\pi_{k-1} v(t)\|^2 dt + \frac{1}{2} \|v(T)\|_0^2 \right)^{1/2}.$$

Note that $\|\cdot\|_{\text{cGP}}$ is on X_h^k not only a semi-norm but a norm. Indeed, the first term inside the definition of $\|\cdot\|_{\text{cGP}}$ guarantees that $\|v\|_{\text{cGP}} = 0$ results in a function v which is on each time interval I_n given by $L_k^{(n)}(t)\varphi(x)$ where $L_k^{(n)}$ is the transformed k -th Legendre polynomial on I_n and $\varphi \in V_h$. Due to $v(T) = 0$ and $L_k^{(N)}(T) = 1$, the function v vanishes on the last time interval I_N . The continuity of v on I gives then $v(t_{N-1}) = 0$. By recursion we obtain that $v \equiv 0$ on I . Hence, $\|\cdot\|_{\text{cGP}}$ is a norm on X_h^k .

We will show in the following lemma a property of the bilinear form B_h which will be used in the next theorem to prove existence, uniqueness, and stability of fully discrete problem (19).

Lemma 3.1. *The condition*

$$\|v_{h,\tau}\|_{\text{cGP}}^2 \leq B_h(v_{h,\tau}, \pi_{k-1}v_{h,\tau}) + \frac{1}{2}\|v_{h,\tau}(0)\|_0^2 \quad (21)$$

holds true for all $v_{h,\tau} \in X_h^k$.

Proof. Using the definition (16) of B_h , we obtain

$$B_h(v_{h,\tau}, \pi_{k-1}v_{h,\tau}) = \int_0^T (v'_{h,\tau}, \pi_{k-1}v_{h,\tau}) + a_h(v_{h,\tau}, \pi_{k-1}v_{h,\tau}) \, dt. \quad (22)$$

We get

$$\int_0^T (v'_{h,\tau}, \pi_{k-1}v_{h,\tau}) \, dt = \int_0^T (v'_{h,\tau}, v_{h,\tau}) \, dt = \frac{1}{2} \int_0^T \frac{d}{dt} \|v_{h,\tau}\|_0^2 \, dt = \frac{1}{2} \|v_{h,\tau}(T)\|_0^2 - \frac{1}{2} \|v_{h,\tau}(0)\|_0^2$$

for the first term on the right-hand side of (22) where the projection property (20) and $v'_{h,\tau} \in Y_h^{k-1}$ were applied. The second term in (22) uses the fact that convection and reaction are independent of time. The definition (20) of π_{k-1} and the coercivity (12) of the bilinear form a_h give

$$\int_0^T a_h(v_{h,\tau}, \pi_{k-1}v_{h,\tau}) \, dt = \int_0^T a_h(\pi_{k-1}v_{h,\tau}, \pi_{k-1}v_{h,\tau}) \, dt \geq \int_0^T \|\pi_{k-1}v_{h,\tau}\|^2 \, dt.$$

Putting all these estimates into (22), we get

$$B_h(v_{h,\tau}, \pi_{k-1}v_{h,\tau}) \geq \int_0^T \|\pi_{k-1}v_{h,\tau}\|^2 \, dt + \frac{1}{2} \|v_{h,\tau}(T)\|_0^2 - \frac{1}{2} \|v_{h,\tau}(0)\|_0^2 = \|v_{h,\tau}\|_{\text{cGP}}^2 - \frac{1}{2} \|v_{h,\tau}(0)\|_0^2. \quad (23)$$

Hence, the statement of this lemma follows. \square

The next theorem states the stability of the fully discrete method (19).

Theorem 3.2. *The solution $u_{h,\tau}$ of the fully discrete problem (19) is uniquely determined and satisfies the stability estimate*

$$\|u_{h,\tau}\|_{\text{cGP}} \leq \frac{1}{\sqrt{\sigma_0}} \left(\int_0^T \|f\|_0^2 \, dt \right)^{1/2} + \|j_h u_0\|_0 \quad (24)$$

with the constant σ_0 from (2).

Proof. Due to Lemma 3.1, we have

$$\begin{aligned} \|u_{h,\tau}\|_{\text{cGP}}^2 &\leq B_h(u_{h,\tau}, \pi_{k-1}u_{h,\tau}) + \frac{1}{2} \|u_{0,h}\|_0^2 = \int_0^T (f, \pi_{k-1}u_{h,\tau}) \, dt + \frac{1}{2} \|u_{0,h}\|_0^2 \\ &\leq \int_0^T \|f\|_0 \|\pi_{k-1}u_{h,\tau}\|_0 \, dt + \frac{1}{2} \|u_{0,h}\|_0^2 \\ &\leq \frac{1}{\sqrt{\sigma_0}} \int_0^T \|f\|_0 \sqrt{\sigma_0} \|\pi_{k-1}u_{h,\tau}\|_0 \, dt + \frac{1}{2} \|u_{0,h}\|_0^2 \\ &\leq \frac{1}{2\sigma_0} \int_0^T \|f\|_0^2 \, dt + \frac{1}{2} \int_0^T \|\pi_{k-1}u_{h,\tau}\|^2 \, dt + \frac{1}{2} \|u_{0,h}\|_0^2 \end{aligned}$$

$$\leq \frac{1}{2\sigma_0} \int_0^T \|f\|_0^2 dt + \frac{1}{2} \|u_{h,\tau}\|_{\text{cGP}}^2 + \frac{1}{2} \|u_{0,h}\|_0^2$$

and the statement of this Lemma follows since $u_{h,\tau}(0) = j_h u(0)$. \square

We define for the sufficiently smooth solution u of (18) its time interpolant $\tilde{u} \in X^k$ on the interval I_n by

$$\tilde{u}(t_{n-1}) = u(t_{n-1}), \quad \tilde{u}(t_n) = u(t_n), \quad \int_{I_n} (u(t) - \tilde{u}(t), w(t)) dt = 0 \quad \forall w \in \mathbb{P}_{k-2}(I_n, V). \quad (25)$$

Hence, the standard interpolation error estimates

$$\int_{I_n} |u(t) - \tilde{u}(t)|_m dt \leq C \tau_n^{k+1} \int_{I_n} |u^{(k+1)}(t)|_m dt, \quad (26)$$

$$\int_{I_n} |(u - \tilde{u})'(t)|_m dt \leq C \tau_n^k \int_{I_n} |u^{(k+1)}(t)|_m dt \quad (27)$$

hold true for $m \in \{0, 1\}$ and all time intervals I_n , $n = 1, \dots, N$.

Theorem 3.3. *Assume $\mu_K \sim h_K$ for all $K \in \mathcal{T}_h$. Suppose A1 and A2. Let $u_{h,\tau}$ and u be the solutions of the fully discrete problem (19) and the continuous problem (18), respectively. Moreover, let $u \in \mathbf{H}^1(\mathbf{H}^{r+1}) \cap \mathbf{H}^{k+1}(\mathbf{H}^1)$. Then, there exists a positive constant C independent of h , τ , and ε , such that the error estimate*

$$\|u_{h,\tau} - u\|_{\text{cGP}} \leq C \left[\tau^{k+1} \|u\|_{\mathbf{H}^{k+1}(\mathbf{H}^1)} + (\varepsilon^{1/2} + h^{1/2}) h^r \|u\|_{\mathbf{H}^1(\mathbf{H}^{r+1})} \right] \quad (28)$$

holds true.

Proof. The error analysis starts by decomposing the error $e := u_{h,\tau} - u$ into the interpolation error $\eta := j_h \tilde{u} - u$ and the difference $\xi := u_{h,\tau} - j_h \tilde{u}$ between discrete solution and the interpolant of u . Hence, we have

$$u_{h,\tau} - u = e = \xi + \eta.$$

Lemma 3.1 for the discrete error function ξ provides

$$\|\xi\|_{\text{cGP}}^2 \leq B_h(\xi, v_{h,\tau}) + \frac{1}{2} \|\xi(0)\|_0^2 = B_h(\xi, \pi_{k-1}\xi) \quad (29)$$

since $\xi(0) = u_{h,\tau}(0) - j_h \tilde{u}(0) = 0$ due to the choice of the discrete initial condition and the properties (25) of the interpolation in time.

In the following, we will bound the right-hand side of (29). We obtain from (18) and (19) the error equation

$$\begin{aligned} B_h(\xi, \pi_{k-1}\xi) &= \int_0^T (f, \pi_{k-1}\xi) dt - \int_0^T ((j_h \tilde{u})', \pi_{k-1}\xi) dt - \int_0^T a_h(j_h \tilde{u}, \pi_{k-1}\xi) dt \\ &= \int_0^T (u', \pi_{k-1}\xi) dt + \int_0^T a(u, \pi_{k-1}\xi) dt - \int_0^T ((j_h \tilde{u})', \pi_{k-1}\xi) dt - \int_0^T a_h(j_h \tilde{u}, \pi_{k-1}\xi) dt \\ &= - \int_0^T (\eta', \pi_{k-1}\xi) dt - \int_0^T a(\eta, \pi_{k-1}\xi) dt - \int_0^T S_h(\eta, \pi_{k-1}\xi) dt - \int_0^T S_h(u, \pi_{k-1}\xi) dt. \end{aligned} \quad (30)$$

The arising terms on the right-hand side of (30) will be bounded by terms depending on the solution u of the continuous problem (18). Using the error splitting and an integration by parts with respect to time, we get

$$- \int_0^T (\eta', \pi_{k-1}\xi) dt = \int_0^T ((u - \tilde{u})', \pi_{k-1}\xi) dt + \int_0^T ((\tilde{u} - j_h \tilde{u})', \pi_{k-1}\xi) dt$$

$$\begin{aligned}
&= \sum_{n=1}^N \left(- \int_{I_n} (u - \tilde{u}, (\pi_{k-1}\xi)') dt + (u - \tilde{u}, \pi_{k-1}\xi) \Big|_{t_{n-1}}^{t_n} \right) + \int_0^T ((\tilde{u} - j_h \tilde{u})', \pi_{k-1}\xi) dt \\
&= \int_0^T (\tilde{u}' - j_h \tilde{u}', \pi_{k-1}\xi) dt.
\end{aligned}$$

Here, we have used the properties (25) of interpolation in time and the fact that time derivative and interpolation in space commute. Hence, using the Cauchy-Schwarz inequality, the interpolation properties of j_h , and the stability property of the interpolation in time, we obtain

$$\begin{aligned}
\left| - \int_0^T (\eta', \pi_{k-1}\xi) dt \right| &\leq \sum_{n=1}^N \int_{I_n} \|\tilde{u}' - j_h \tilde{u}'\|_0 \|\pi_{k-1}\xi\|_0 dt \leq Ch^{r+1} \sum_{n=1}^N \int_{I_n} \|\tilde{u}'\|_{r+1} \|\pi_{k-1}\xi\|_0 dt \\
&\leq Ch^{r+1} \left(\sum_{n=1}^N \int_{I_n} \|\tilde{u}'\|_{r+1}^2 dt \right)^{1/2} \left(\sum_{n=1}^N \int_{I_n} \sigma_0 \|\pi_{k-1}\xi\|_0^2 dt \right)^{1/2} \\
&\leq Ch^{r+1} \|u\|_{\mathbf{H}^1(\mathbf{H}^{r+1})} \|\xi\|_{\text{cGP}}.
\end{aligned}$$

To get an estimate for the second term on the right-hand side of (30), we exploit the definition of the bilinear form a . Using the Cauchy-Schwarz inequality, the error splitting, and the approximation properties (8) and (26), we get

$$\begin{aligned}
&\left| \int_0^T \left\{ \varepsilon(\nabla\eta, \nabla\pi_{k-1}\xi) + (\sigma\eta, \pi_{k-1}\xi) \right\} dt \right| \\
&\leq C \sum_{n=1}^N \int_{I_n} (\varepsilon|u - j_h \tilde{u}|_1^2 + \|u - j_h \tilde{u}\|_0^2)^{1/2} \|\pi_{k-1}\xi\| dt \\
&\leq C \sum_{n=1}^N \int_{I_n} \left(\varepsilon|u - \tilde{u}|_1^2 + \varepsilon|\tilde{u} - j_h \tilde{u}|_1^2 + \|u - \tilde{u}\|_0^2 + \|\tilde{u} - j_h \tilde{u}\|_0^2 \right)^{1/2} \|\pi_{k-1}\xi\| dt \\
&\leq C \sum_{n=1}^N \left[\int_{I_n} \left((\varepsilon + h^2)h^{2r} \|\tilde{u}\|_{r+1}^2 + (\varepsilon + 1)\tau_n^{2(k+1)} \left(\|u^{(k+1)}\|_0^2 + |u^{(k+1)}|_1^2 \right) \right)^{1/2} \|\pi_{k-1}\xi\| dt \right] \\
&\leq C \left[(\varepsilon^{1/2} + h)h^r \|u\|_{\mathbf{L}^2(\mathbf{H}^{r+1})} + (\varepsilon^{1/2} + 1)\tau^{k+1} \|u\|_{\mathbf{H}^{k+1}(\mathbf{H}^1)} \right] \|\xi\|_{\text{cGP}}.
\end{aligned}$$

In order to estimate the convection term in the bilinear form a , we proceed as follows. Using the error splitting, we get

$$\int_0^T (\mathbf{b} \cdot \nabla\eta, \pi_{k-1}\xi) dt = - \int_0^T (\mathbf{b} \cdot \nabla(u - \tilde{u}), \pi_{k-1}\xi) dt - \int_0^T (\mathbf{b} \cdot \nabla(\tilde{u} - j_h \tilde{u}), \pi_{k-1}\xi) dt. \quad (31)$$

The interpolation error estimate (26) gives for the first term in (31)

$$\begin{aligned}
\left| - \int_0^T (\mathbf{b} \cdot \nabla(u - \tilde{u}), \pi_{k-1}\xi) dt \right| &\leq \frac{\|\mathbf{b}\|_{0,\infty}}{\sqrt{\sigma_0}} \sum_{n=1}^N \int_{I_n} \|\nabla(u - \tilde{u})\|_0 \sqrt{\sigma_0} \|\pi_{k-1}\xi\|_0 dt \\
&\leq C \left(\sum_{n=1}^N \tau_n^{2k+2} \int_{I_n} |u^{(k+1)}|_1^2 dt \right)^{1/2} \left(\sum_{n=1}^N \int_{I_n} \|\pi_{k-1}\xi\|_0^2 dt \right)^{1/2}
\end{aligned}$$

$$\leq C\tau^{k+1}\|u\|_{\mathbb{H}^{k+1}(\mathbb{H}^1)}\|\xi\|_{\text{cGP}}.$$

Integrating the second term in (31) by parts in space gives

$$\left| -\int_0^T (\mathbf{b} \cdot \nabla(\tilde{u} - j_h \tilde{u}), \pi_{k-1} \xi) dt \right| \leq \left| \int_0^T (\tilde{u} - j_h \tilde{u}, \mathbf{b} \cdot \nabla \pi_{k-1} \xi) dt \right| + \left| \int_0^T ((\pi_{k-1} \xi) \operatorname{div} \mathbf{b}, \tilde{u} - j_h \tilde{u}) dt \right|. \quad (32)$$

The first term in (32) is estimated by using the orthogonality condition (9) as follows

$$\begin{aligned} \left| \int_0^T (\tilde{u} - j_h \tilde{u}, \mathbf{b} \cdot \nabla \pi_{k-1} \xi) dt \right| &= \left| \int_0^T \sum_{K \in \mathcal{T}_h} (\tilde{u} - j_h \tilde{u}, \kappa_K (\mathbf{b} \cdot \nabla \pi_{k-1} \xi))_K dt \right| \\ &\leq \int_0^T \sum_{K \in \mathcal{T}_h} \|\tilde{u} - j_h \tilde{u}\|_{0,K} \|\kappa_K (\mathbf{b} \cdot \nabla \pi_{k-1} \xi)\|_{0,K} dt. \end{aligned}$$

One can obtain for $\mathbf{b}|_K \in (W^{1,\infty}(K))^d$ the estimate

$$\|\kappa_K (\mathbf{b} \cdot \nabla \pi_{k-1} \xi)\|_{0,K} \leq C \|\mathbf{b}\|_{1,\infty,K} \|\pi_{k-1} \xi\|_{0,K} + \|\mathbf{b}\|_{0,\infty,K} \|\kappa_K (\nabla \pi_{k-1} \xi)\|_{0,K},$$

see [28, Corollary 2.14]. Using this estimate, the approximation property (8), $\mu_K \sim h_K$, and the stability property of the interpolation in time, we get

$$\begin{aligned} \left| \int_0^T (\tilde{u} - j_h \tilde{u}, \mathbf{b} \cdot \nabla \pi_{k-1} \xi) dt \right| &\leq C \int_0^T \sum_{K \in \mathcal{T}_h} h_K^{r+1} \|\tilde{u}\|_{r+1,K} \left(\|\pi_{k-1} \xi\|_{0,K} + \|\kappa_K (\nabla \pi_{k-1} \xi)\|_{0,K} \right) dt \\ &\leq C \left(\int_0^T \sum_{K \in \mathcal{T}_h} h_K^{2r+2} \|\tilde{u}\|_{r+1,K}^2 dt \right)^{1/2} \left(\int_0^T \sigma_0 \|\pi_{k-1} \xi\|_0^2 dt \right)^{1/2} \\ &\quad + C \left(\int_0^T \sum_{K \in \mathcal{T}_h} \mu_K^{-1} h_K^{2r+2} \|\tilde{u}\|_{r+1,K}^2 dt \right)^{1/2} \left(\int_0^T \sum_{K \in \mathcal{T}_h} \mu_K \|\kappa_K (\nabla \pi_{k-1} \xi)\|_{0,K}^2 dt \right)^{1/2} \\ &\leq Ch^{r+1/2} \|u\|_{L^2(\mathbb{H}^{r+1})} \|\xi\|_{\text{cGP}}. \end{aligned}$$

Using the Cauchy-Schwarz inequality and the properties of the spatial interpolation, we obtain for the second term on the right-hand side of (32)

$$\begin{aligned} \left| \int_0^T ((\pi_{k-1} \xi) \operatorname{div} \mathbf{b}, \tilde{u} - j_h \tilde{u}) dt \right| &\leq C \int_0^T \sum_{K \in \mathcal{T}_h} \|\tilde{u} - j_h \tilde{u}\|_0 \sigma_0^{1/2} \|\pi_{k-1} \xi\|_0 dt \\ &\leq Ch^{r+1} \|u\|_{L^2(\mathbb{H}^{k+1})} \|\xi\|_{\text{cGP}}. \end{aligned}$$

Inserting these estimates into (31), we get

$$\left| \int_0^T (\mathbf{b} \cdot \nabla \eta, \pi_{k-1} \xi) dt \right| \leq C \left[h^{r+1/2} \|u\|_{L^2(\mathbb{H}^{r+1})} + \tau^{k+1} \|u\|_{\mathbb{H}^{k+1}(\mathbb{H}^1)} \right] \|\xi\|_{\text{cGP}}.$$

Hence, we have for the second term on the right-hand side of (30) the following estimate

$$\left| \int_0^T a(\eta, \pi_{k-1} \xi) dt \right| \leq C \left[(\varepsilon^{1/2} + h^{1/2}) h^r \|u\|_{L^2(\mathbb{H}^{r+1})} + \tau^{k+1} \|u\|_{\mathbb{H}^{k+1}(\mathbb{H}^1)} \right]. \quad (33)$$

We rewrite the third term in (30) by using the error splitting as

$$-\int_0^T S_h(\eta, \pi_{k-1}\xi) dt = \int_0^T S_h(u - \tilde{u}, \pi_{k-1}\xi) dt + \int_0^T S_h(\tilde{u} - j_h\tilde{u}, \pi_{k-1}\xi) dt. \quad (34)$$

Then, the stability of the fluctuation operator κ_K , the boundedness of μ_K , and the error estimates of the interpolation in time give for the first term in (34)

$$\begin{aligned} \left| \int_0^T S_h(u - \tilde{u}, \pi_{k-1}\xi) dt \right| &\leq \sum_{n=1}^N \int_{I_n} S_h^{1/2}(u - \tilde{u}, u - \tilde{u}) S_h^{1/2}(\pi_{k-1}\xi, \pi_{k-1}\xi) dt \\ &\leq \sum_{n=1}^N \int_{I_n} \left(\sum_{K \in \mathcal{T}_h} \mu_K \|\kappa_K \nabla(u - \tilde{u})\|_{0,K}^2 \right)^{1/2} \|\pi_{k-1}\xi\| dt \\ &\leq C\tau^{k+1} \|u\|_{\mathbf{H}^{k+1}(\mathbf{H}^1)} \|\xi\|_{\text{cGP}}. \end{aligned}$$

Similarly, the L^2 -stability of the fluctuation operator κ_K , the parameter choice $\mu_K \sim h_K$, and (8) result for the second term of (34) in

$$\begin{aligned} \left| \int_0^T S_h(\tilde{u} - j_h\tilde{u}, \pi_{k-1}\xi) dt \right| &\leq \int_0^T S_h^{1/2}(\tilde{u} - j_h\tilde{u}, \tilde{u} - j_h\tilde{u}) S_h^{1/2}(\pi_{k-1}\xi, \pi_{k-1}\xi) dt \\ &\leq \int_0^T \left(\sum_{K \in \mathcal{T}_h} \mu_K \|\kappa_K(\nabla(\tilde{u} - j_h\tilde{u}))\|_{0,K}^2 \right)^{1/2} \|\pi_{k-1}\xi\| dt \\ &\leq Ch^{r+1/2} \int_0^T \|\tilde{u}\|_{r+1} \|\pi_{k-1}\xi\| dt \leq Ch^{r+1/2} \|u\|_{L^2(\mathbf{H}^{r+1})} \|\xi\|_{\text{cGP}}. \end{aligned}$$

Hence, we get

$$\left| -\int_0^T S_h(\eta, \pi_{k-1}\xi) dt \right| \leq C(h^{r+1/2} \|u\|_{L^2(\mathbf{H}^{r+1})} + \tau^{k+1} \|u\|_{\mathbf{H}^{k+1}(\mathbf{H}^1)}) \|\xi\|_{\text{cGP}}. \quad (35)$$

To estimate the last term in (30), we use the Cauchy-Schwarz inequality, the approximation properties of the fluctuation operator κ_K , and the parameter choice $\mu_K \sim h_K$ to get

$$\begin{aligned} \left| \int_0^T S_h(u, \pi_{k-1}\xi) dt \right| &\leq \int_0^T S_h^{1/2}(u, u) S_h^{1/2}(\pi_{k-1}\xi, \pi_{k-1}\xi) dt \leq C \int_0^T \left(\sum_{K \in \mathcal{T}_h} \mu_K \|\kappa_K(\nabla u)\|_{0,K}^2 \right)^{1/2} \|\pi_{k-1}\xi\| dt \\ &\leq Ch^{r+1/2} \|u\|_{L^2(\mathbf{H}^{r+1})} \|\xi\|_{\text{cGP}}. \end{aligned} \quad (36)$$

Putting the above estimates into (30), we obtain

$$B_h(u_{h,\tau} - j_h\tilde{u}, \pi_{k-1}\xi) \leq C \left[(\varepsilon^{1/2} + h^{1/2}) h^r \|u\|_{\mathbf{H}^1(\mathbf{H}^{r+1})} + \tau^{k+1} \|u\|_{\mathbf{H}^{k+1}(\mathbf{H}^1)} \right] \|\xi\|_{\text{cGP}}.$$

Using (29), it follows that

$$\|u_{h,\tau} - j_h\tilde{u}\|_{\text{cGP}} \leq C \left[(\varepsilon^{1/2} + h^{1/2}) h^r \|u\|_{\mathbf{H}^1(\mathbf{H}^{r+1})} + \tau^{k+1} \|u\|_{\mathbf{H}^{k+1}(\mathbf{H}^1)} \right].$$

Finally, the statement of this Theorem follows by applying the triangle inequality and the interpolation error estimates in space and time. \square

The next theorem gives an $L^2(L^2)$ error estimate for the error $u - u_{h,\tau}$ which is optimal with respect to time.

Theorem 3.4. *Assume $\mu_K \sim h_K$ for all $K \in \mathcal{T}_h$. Suppose A1 and A2. Let $u_{h,\tau}$ and u be the solutions of the fully discrete problem (19) and the continuous problem (18), respectively. Moreover, let $u \in \mathbf{H}^1(\mathbf{H}^{r+1}) \cap \mathbf{H}^{k+1}(\mathbf{H}^1)$. Then, there exists a positive constant C independent of h , τ , and ε , such that the error estimate*

$$\left(\int_0^T \|u(t) - u_{h,\tau}(t)\|_0^2 dt \right)^{1/2} \leq C \left[\tau^{k+1} \|u\|_{\mathbf{H}^{k+1}(\mathbf{H}^1)} + (\varepsilon^{1/2} + h^{1/2}) h^r \|u\|_{\mathbf{H}^1(\mathbf{H}^{r+1})} \right] \quad (37)$$

holds true.

Proof. Let $e = u_{h,\tau} - u$ be the error. Applying the ideas of the proof of Theorem 3.3 not only on $[0, T]$ but also on $[0, t_n]$, $n = 1, \dots, N-1$, results in the estimate

$$\int_0^{t_n} \|\pi_{k-1} e(t)\|_0^2 dt + \frac{1}{2} \|e(t_n)\|_0^2 \leq C \left[\tau^{2(k+1)} \|u\|_{\mathbf{H}^{k+1}(\mathbf{H}^1)}^2 + (\varepsilon + h) h^{2r} \|u\|_{\mathbf{H}^1(\mathbf{H}^{r+1})}^2 \right]$$

where the ranges of the time integrals on the right-hand side were extended from $[0, t_n]$ to $[0, T]$ due to the monotonicity of the integrals. Neglecting the non-negative integral of the left-hand side, a summation over $n = 1, \dots, N$ provides

$$\frac{\tau}{2} \sum_{n=1}^N \|e(t_n)\|_0^2 \leq C \left[\tau^{2(k+1)} \|u\|_{\mathbf{H}^{k+1}(\mathbf{H}^1)}^2 + (\varepsilon + h) h^{2r} \|u\|_{\mathbf{H}^1(\mathbf{H}^{r+1})}^2 \right]$$

which together with Thm. 3.3 gives

$$\left(\int_0^T \|\pi_{k-1} e(t)\|_0^2 dt + \frac{\tau}{2} \sum_{n=1}^N \|e(t_n)\|_0^2 \right)^{1/2} \leq C \left[\tau^{k+1} \|u\|_{\mathbf{H}^{k+1}(\mathbf{H}^1)} + (\varepsilon^{1/2} + h^{1/2}) h^r \|u\|_{\mathbf{H}^1(\mathbf{H}^{r+1})} \right]. \quad (38)$$

To get an $L^2(L^2)$ estimate for the error itself, we split the error

$$\int_0^T \|e(t)\|_0^2 dt \leq 2 \int_0^T \|u_{h,\tau}(t) - \tilde{u}(t)\|_0^2 dt + 2 \int_0^T \|\tilde{u}(t) - u\|_0^2 dt. \quad (39)$$

The second term can be bounded as follows

$$2 \int_0^T \|\tilde{u}(t) - u(t)\|_0^2 dt \leq C \tau^{2(k+1)} \int_0^T \|u^{(k+1)}(t)\|_0^2 dt$$

where the interpolation error estimate (26) was used. Let $e_\tau := u_{h,\tau} - \tilde{u}$ and note that e_τ is a piece-wise \mathbb{P}_k -polynomial in time. Due to the norm equivalence on finite dimensional spaces, we have

$$\int_{t_{n-1}}^{t_n} \|e_\tau(t)\|_0^2 dt \leq C \left(\int_{t_{n-1}}^{t_n} \|\pi_{k-1} e_\tau(t)\|_0^2 dt + \tau_n \|e_\tau(t_n)\|_0^2 \right). \quad (40)$$

Using $e_\tau(t_n) = u_{h,\tau}(t_n) - \tilde{u}(t_n)$ and $\tilde{u}(t_n) = u(t_n)$ due to the definition of the time interpolation, we obtain

$$\tau_n \|e_\tau(t_n)\|_0^2 = \tau_n \|u_{h,\tau}(t_n) - u(t_n)\|_0^2 \leq C \left(\tau^{2(k+1)} \|u\|_{\mathbf{H}^{k+1}(\mathbf{H}^1)}^2 + (\varepsilon + h) h^{2r} \|u\|_{\mathbf{H}^1(\mathbf{H}^{r+1})}^2 \right) \quad (41)$$

where (38) was used. In order to estimate the projection term in (40), we proceed as follows

$$\int_{t_{n-1}}^{t_n} \|\pi_{k-1} e_\tau(t)\|_0^2 dt \leq 2 \int_{t_{n-1}}^{t_n} \|\pi_{k-1}(u_{h,\tau} - u)(t)\|_0^2 dt + 2 \int_{t_{n-1}}^{t_n} \|\pi_{k-1}(u - \tilde{u})(t)\|_0^2 dt. \quad (42)$$

The first term can be bounded using Thm. 3.3. To estimate the second term in (42), the stability of the L^2 -projection π_{k-1} and the interpolation estimates (26) in time are applied. We obtain

$$\int_{t_{n-1}}^{t_n} \|\pi_{k-1}(u - \tilde{u})(t)\|_0^2 dt \leq C\tau_n^{2(k+1)} \int_{t_{n-1}}^{t_n} \|u^{(k+1)}(t)\|_0^2 dt.$$

Putting together all above estimates, the $L^2(L^2)$ bound

$$\left(\int_0^T \|e(t)\|_0^2 dt \right)^{1/2} \leq C \left[\tau^{k+1} \|u\|_{\mathbf{H}^{k+1}(\mathbf{H}^1)} + (\varepsilon^{1/2} + h^{1/2}) h^r \|u\|_{\mathbf{H}^1(\mathbf{H}^{r+1})} \right] \quad (43)$$

is obtained. \square

3.2. The discontinuous Galerkin (dG) method

We describe in this subsection briefly of the discontinuous Galerkin (dG) time discretization in combination with the LPS method in space. Let us introduce the bilinear form B_h^{dG} by

$$B_h^{\text{dG}}(u, v) := \sum_{n=1}^N \int_{I_n} \left\{ (u'(t), v(t)) + a_h(u(t), v(t)) \right\} dt + \sum_{n=1}^{N-1} ([u]_n, v_n^+) + (u_0^+, v_0^+) \quad (44)$$

where the jumps $[\varphi]_n$ and the right-sided values φ_n^+ are defined in (14). The linear form l^{dG} is given by

$$l^{\text{dG}}(v) := (u_0, v_0^+) + \int_0^T (f(t), v(t)) dt. \quad (45)$$

The fully discrete scheme reads:

Find $u_{h,\tau} \in Y_h^k$ such that

$$B_h^{\text{dG}}(u_{h,\tau}, v_{h,\tau}) = l^{\text{dG}}(v_{h,\tau}) \quad \forall v_{h,\tau} \in Y_h^k. \quad (46)$$

The mesh-dependent norm is defined by

$$\|v\|_{\text{dG}} := \left(\sum_{n=1}^N \int_{I_n} \|v(t)\|^2 dt + \frac{1}{2} \|v_0^+\|_0^2 + \frac{1}{2} \sum_{n=1}^{N-1} \|[v]_n\|_0^2 + \frac{1}{2} \|v_N^-\|_0^2 \right)^{1/2}. \quad (47)$$

The next theorem cites the main results from [2] where the local projection stabilization method in space has been combined with the discontinuous Galerkin method in time.

Theorem 3.5. *Suppose A1, A2, and $\mu_K \sim h_K$ for all $K \in \mathcal{T}_h$. Let $u_{h,\tau}$ and u be the solutions of the fully discrete scheme (46) and the continuous problem (4), respectively. Moreover, let $u \in \mathbf{H}^1(\mathbf{H}^{r+1}) \cap \mathbf{H}^{k+1}(\mathbf{H}^1)$. Then, there exists a positive constant C independent of h , τ , and ε , such that the error estimate*

$$\|u_{h,\tau} - u\|_{\text{dG}} \leq C\tau^{k+1/2} \|u\|_{\mathbf{H}^{k+1}(\mathbf{H}^1)} + C(\varepsilon^{1/2} + h^{1/2}) h^r \left(\|u\|_{\mathbf{H}^1(\mathbf{H}^{r+1})} + \|u\|_{\mathbf{C}(\mathbf{H}^{k+1})} \right) \quad (48)$$

holds true.

4. NUMERICAL STUDIES

We present in this section some numerical experiments to assess accuracy and performance of local projection stabilization techniques in space combined with higher order variational time discretization schemes. All computations have been performed using MooNMD [21].

In our numerical computations, we have used mapped finite element spaces [10] where the enriched spaces on the reference cell \widehat{K} are given by

$$\begin{aligned}\mathbb{P}_r^{\text{bubble}}(\widehat{K}) &:= \mathbb{P}_r(\widehat{K}) + \hat{b}_\Delta \mathbb{P}_{r-1}(\widehat{K}), & r \geq 1, \\ \mathbb{Q}_r^{\text{bubble}}(\widehat{K}) &:= \mathbb{Q}_r(\widehat{K}) + \text{span}\{\hat{b}_\square \hat{x}_i^{r-1}, i = 1, 2\}, & r \geq 1.\end{aligned}$$

Here, \hat{b}_Δ and \hat{b}_\square are the cubic bubble function on the reference triangle and the biquadratic bubble function on the reference square, respectively. The mapped finite element spaces based on $\mathbb{P}_r^{\text{bubble}}(\widehat{K})$ and $\mathbb{Q}_r^{\text{bubble}}(\widehat{K})$ will be shortly denoted by $\mathbb{P}_r^{\text{bubble}}$ and $\mathbb{Q}_r^{\text{bubble}}$, respectively.

The combinations $V_h = \mathbb{P}_r^{\text{bubble}}$, $D(K) = \mathbb{P}_{r-1}(K)$, $r \geq 1$, on triangular meshes and the combinations $V_h = \mathbb{Q}_r^{\text{bubble}}$, $D(K) = \mathbb{P}_{r-1}(K)$, $r \geq 1$, on quadrilateral meshes fulfill the assumptions A1 and A2. Further examples of approximation spaces V_h and projection spaces $D(K)$ satisfying A1 and A2 are given in [28, 31].

The stabilization parameters μ_K have been chosen as

$$\mu_K = \mu_0 h_K \quad \forall K \in \mathcal{T}_h$$

where μ_0 denotes a positive constant which will be given for each of the test calculations.

We define by

$$\|v\|_{L^2(L^2)} := \left\{ \int_0^T \|v(t)\|_0^2 dt \right\}^{1/2}, \quad \|v\|_\infty := \max_{1 \leq n \leq N} \|v(t_n)\|_0$$

the $L^2(L^2)$ -norm and the discrete $\ell^\infty(L^2)$ -norm in time.

Example 1. The rotating Gaussian benchmark as a pure transport problem in two space dimensions is taken from [2, 9]. Hence, we consider the problem (1) in

$$\Omega = \{(x, y) \in \mathbb{R}^2 : x^2 + y^2 < 1\}$$

with the data

$$\varepsilon = 0, \quad b = (-y, x)^T, \quad \sigma = f = 0, \quad T = 2\pi,$$

and the Gaussian initial condition

$$u_0(x, y) = \exp\left(-10(x - 0.3)^2 - 10(y - 0.3)^2\right)$$

which is centered at (0.3, 0.3). Note that the solution u is at all times given by a suitably rotated initial condition.

The calculations have been performed on triangular meshes which were obtained from an initial triangulation by successive refinement with boundary adaption due to the curved boundary. The initial mesh (level 0) and the mesh on level 3 are shown in Fig. 1.

In this example, we are interested in the convergence order in space. To this end, we keep the error in time small by using the methods cGP(3) and dG(2) with time step length $\tau = 2\pi \cdot 10^{-3}$. Hence, 1000 time steps correspond to one complete revolution of the Gaussian. We used the LPS discretizations with $V_h = \mathbb{P}_3^{\text{bubble}}$, $D(K) = \mathbb{P}_2(K)$, and the stabilization parameters $\mu_K = 0.1h_K$. Table 1 shows for the time discretizations cGP(3) and dG(2) the errors and convergence orders in the cGP-norm and the dG-norm. It is clearly to see that the convergence orders predicted by Thm. 3.3 are achieved. Moreover, the differences between the two

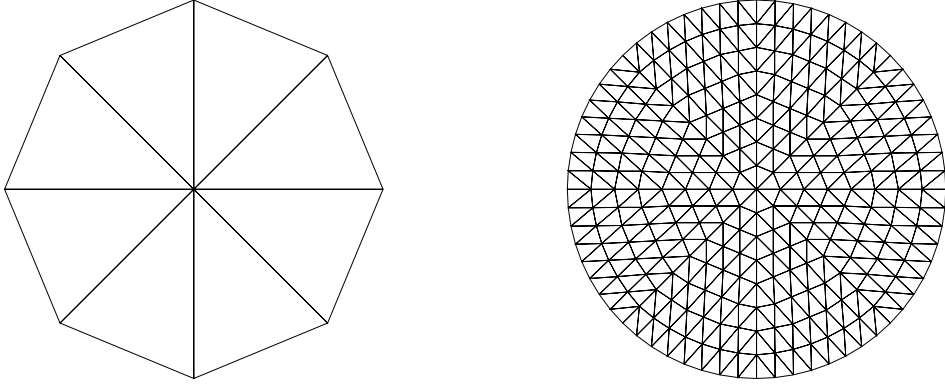


FIGURE 1. Triangular meshes for Example 1: coarsest mesh (left) and mesh after three refinement steps (right).

time discretization schemes are very small. This is due to the fact that the temporal error is almost eliminated by the used higher order time discretizations with small time step length.

TABLE 1. Example 1: errors and convergence orders in space for cGP(3) and dG(2).

Level	$\ u - u_{h,\tau}\ _{\text{cGP}}$ cGP(3)		$\ u - u_{h,\tau}\ _{\text{dG}}$ dG(2)	
	error	order	error	order
2	7.892-2		7.900-2	
3	8.234-3	3.26	8.238-3	3.26
4	7.001-4	3.56	7.003-4	3.56
5	6.192-5	3.50	6.192-5	3.50
6	5.471-6	3.50	5.473-6	3.50
theory		3.5		3.5

Example 2. In order to assess the effect of the applied time discretizations, we exclude in this example the spatial error. We consider problem (1) in $\Omega = (0, 1)^2$ with $\varepsilon = 10^{-8}$, $\mathbf{b} = (1, 2)$, $\sigma = 1$, and $T = 1$. The right-hand side f and the initial condition u_0 are chosen such that

$$u(x, y, t) = 1 + 2x + 3t^{200}y$$

is the solution of (1) equipped with non-homogeneous Dirichlet boundary conditions.

We used the LPS discretizations with $V_h = \mathbb{Q}_1^{\text{bubble}}$, $D(K) = \mathbb{P}_0(K)$, and stabilization parameter $\mu_K = 0.1h_K$. A uniform mesh consisting of 4×4 squares was considered in our calculations. Note that for any time t the solution u can be represented exactly by a function from the finite element space V_h . Hence, all occurring errors will result from the temporal discretizations. The higher order time discretization methods cGP(3), cGP(4) and dG(2), dG(3) were applied.

We report in Tab. 2-3 the errors and convergence orders for these methods. We see that all considered methods are accurate of order $k + 1$ in the $L^2(L^2)$ -norm as predicted by Thm. 3.4. The orders $k + 1$ and $k + 1/2$ in the cGP-norm and the dG-norm are achieved which also confirms the theoretical results. The values in the discrete $\ell^\infty(L^2)$ -norms show clearly that the cGP(k)-methods, $k = 3, 4$, are super-convergent of order $2k$ while the dG(k)-methods, $k = 2, 3$, are super-convergent of order $2k + 1$. These superconvergence results are known for the heat equation, see [3, 35].

Table 4 shows the error $e = u - \Pi u_{h,\tau}$ in the $L^2(L^2)$ -norm where $\Pi u_{h,\tau}$ denotes the post-processed solution which is obtained by means of a simple post-processing from the solution $u_{h,\tau}$ of the original cGP-method or dG-method. Details of the post-processing can be found in [1, 27]. Note that the post-processed solutions of both cGP(k) and dG(k) are super-convergent of order $k + 2$ in the $L^2(L^2)$ -norm. This is confirmed by the error norms in Table 4.

TABLE 2. Example 2: errors and convergence orders for cGP(3) and dG(2).

τ	$\ u - u_{h,\tau}\ _{L^2(L^2)}$				$\ u - u_{h,\tau}\ _\infty$				$\ u - u_{h,\tau}\ _{\text{cGP}}$		$\ u - u_{h,\tau}\ _{\text{dG}}$	
	cGP(3)		dG(2)		cGP(3)		dG(2)		cGP(3)		dG(2)	
	error	order	error	order	error	order	error	order	error	order	error	order
1/20	5.028-2		1.415-1		1.655-1		4.296-1		6.766-1		1.189	
1/40	8.130-3	2.63	3.453-2	2.04	8.821-3	4.23	4.047-2	3.40	1.164-1	2.53	4.565-1	1.38
1/80	8.336-4	3.28	6.038-3	2.52	2.230-4	1.82	1.950-3	0.87	1.282-2	3.18	1.227-1	1.90
1/160	6.340-5	3.71	8.364-4	2.85	1.350-5	7.53	2.325-4	6.57	1.003-3	3.68	2.497-2	2.29
1/320	4.205-6	3.91	1.055-4	2.99	6.531-8	7.69	2.215-6	6.71	6.704-5	3.90	4.517-3	2.47
1/640	2.670-7	3.97	1.305-5	3.00	1.030-9	5.99	6.958-8	4.99	4.265-6	3.97	7.945-4	2.50
theory		4		3		6		5		4		2.5

TABLE 3. Example 2: errors and convergence orders for cGP(4) and dG(3).

τ	$\ u - u_{h,\tau}\ _{L^2(L^2)}$				$\ u - u_{h,\tau}\ _\infty$				$\ u - u_{h,\tau}\ _{\text{cGP}}$		$\ u - u_{h,\tau}\ _{\text{dG}}$	
	cGP(4)		dG(3)		cGP(4)		dG(3)		cGP(4)		dG(3)	
	error	order	error	order	error	order	error	order	error	order	error	order
1/20	1.682-2		5.201-2		1.510-2		4.925-2		3.103-1		5.381-1	
1/40	1.659-3	3.34	8.285-3	2.65	2.247-4	6.07	1.368-3	5.17	3.276-2	3.24	1.339-1	2.00
1/80	9.414-5	4.14	8.293-4	3.32	1.599-5	3.81	1.916-4	2.84	1.934-3	4.08	2.005-2	2.74
1/160	3.704-6	4.67	6.088-5	3.77	2.201-8	9.50	5.182-6	8.53	7.705-5	4.65	2.130-3	3.23
1/320	1.240-7	4.90	3.930-6	3.95	2.683-11	9.67	1.257-9	8.69	2.587-6	4.90	1.961-4	3.44
1/640	3.945-9	4.97	2.456-7	4.00	2.295-13	6.52	9.657-11	7.02	8.240-8	4.97	1.738-5	3.49
theory		5		4		8		7		5		3.5

TABLE 4. Example 2: errors and convergence orders of post-processed solution for cGP(3), cGP(4), dG(2), and dG(3).

τ	$\ u - \Pi u_{h,\tau}\ _{L^2(L^2)}$				$\ u - \Pi u_{h,\tau}\ _{L^2(L^2)}$			
	cGP(3)		cGP(4)		dG(2)		dG(3)	
	error	order	error	order	error	order	error	order
1/20	3.834-2		1.200-2		1.049-1		3.675-2	
1/40	4.566-3	3.07	7.620-4	3.98	1.826-2	2.52	3.706-3	3.31
1/80	2.786-4	4.04	2.363-5	5.00	2.936-3	3.24	2.063-4	4.17
1/160	1.115-5	4.64	4.750-7	5.64	1.451-4	3.73	7.886-6	4.71
1/320	3.740-7	4.90	8.978-9	5.90	9.435-6	3.94	2.586-7	4.93
1/640	1.190-8	4.97	1.270-10	5.97	6.911-7	4.00	8.130-9	4.99
theory		5		6		4		5

Example 3. This example is taken from [23]. The prescribed solution has the form

$$u(x, y, t) = 16 \sin(\pi t) x(1-x)y(1-y) \left(\frac{1}{2} + \frac{\arctan [2\varepsilon^{-1/2} w(x, y)]}{\pi} \right) \quad (49)$$

where

$$w(x, y) := 0.25^2 - (x - 0.5)^2 - (y - 0.5)^2.$$

This is a hump which changes its height in the course of time. The steepness of the circular internal layer depends on the diffusion parameter ε . Analogue to [23], we present the simulation for $\Omega = (0, 1)^2$, $\varepsilon = 10^{-6}$, $\mathbf{b} = (2, 3)$, $\sigma = 1$, and $T = 2$. We use

$$\text{var}(t) := \max_{(x,y) \in \Omega} u_{h,\tau}(x, y, t) - \min_{(x,y) \in \Omega} u_{h,\tau}(x, y, t)$$

as a measure for undershoots and overshoots. For calculating the minimal and maximal values of $u_{h,\tau}$, we used only the values at the vertices of the underlying mesh. For evaluating the size of the spurious oscillations, we assess the variation of the discrete solutions $u_{h,\tau}$ at $t = 0.5$ where the hump reaches its maximal height. The exact value is $\text{var}(0.5) = 0.997453575$. Furthermore, some indication of the smearing of the solution is derived from

$$\|e\|_{L^2(V_h)} := \left(\int_0^T \left(\|e(t)\|_0^2 + \varepsilon \|e(t)\|_1^2 \right) dt \right)^{1/2}, \quad e = u - u_{h,\tau}.$$

The time step length was chosen to be $\tau = 10^{-3}$. The computations were performed on a uniform grid consisting of 128×128 squares. This leads to 98,817 degrees of freedom for the spatial discretization with $V_h = \mathbb{Q}_2^{\text{bubble}}$, $D(K) = \mathbb{P}_1(K)$ and 180,993 degrees of freedom for $V_h = \mathbb{Q}_3^{\text{bubble}}$, $D(K) = \mathbb{P}_2(K)$ including the Dirichlet degrees of freedom. Note that in the following figures only the nodal values at the mesh vertices are shown, i.e., the additional bubble part of the solution will not be presented. We have performed calculations with $\mu_0 \in \{0.01, 0.1, 1.0\}$.

The results for cGP(2) with $V_h = \mathbb{Q}_2^{\text{bubble}}$, $D(K) = \mathbb{P}_1(K)$ and cGP(3) with $V_h = \mathbb{Q}_3^{\text{bubble}}$, $D(K) = \mathbb{P}_2(K)$ are presented in Table 5 and in Fig. 2. It can be observed that small and large coefficients μ_0 inside the definition $\mu_K = \mu_0 h_K$ lead to spurious oscillations behind the hump in the direction of convection. The solution obtained by cGP(2) with $\mu_0 = 0.1$ possesses still small overshoots and undershoots whereas the numerical solution obtained by cGP(3) captured very well the solution. Furthermore, almost no oscillations are present.

We visualize in Fig. 3 the computed profiles of the solution for dG(2) with $V_h = \mathbb{Q}_2^{\text{bubble}}$, $D(K) = \mathbb{P}_1(K)$ and dG(3) with $V_h = \mathbb{Q}_3^{\text{bubble}}$, $D(K) = \mathbb{P}_2(K)$. The coefficient μ_0 took the values 0.01, 0.1, and 1. It can be noted that there are no significant differences between the solution obtained by dG(k) and cGP(k), see Tab. 5. Furthermore, the spurious oscillations vanish almost completely also for dG(3).

TABLE 5. Example 3: errors and variation of solutions for cGP(2), cGP(3), dG(2), and dG(3).

μ_0	$\ u - u_{h,\tau}\ _{L^2(V_h)}$				$\text{var}(0.5)$			
	cGP(2)	cGP(3)	dG(2)	dG(3)	cGP(2)	cGP(3)	dG(2)	dG(3)
0.01	7.3575-3	5.5714-3	7.3575-3	5.5714-3	3.3597-2	4.3397-2	3.9573-2	4.3397-2
0.1	4.4980-3	3.2775-3	4.9799-3	1.8913-3	1.8605-2	1.7010-2	1.8605-2	1.7010-2
1.0	6.7158-3	4.7016-3	6.7158-3	4.7016-3	2.7546-2	2.9773-2	2.7546-2	2.9773-2

5. CONCLUSIONS

We have combined higher order variational time discretization by continuous Galerkin–Petrov methods and discontinuous Galerkin methods with the one-level local projection stabilization technique in space. Error estimates for the cGP(k)-method are given and proved. The numerical experiments support the theoretical results. Both time discretization schemes allow to get highly accurate numerical solution. Due to the applied spatial stabilization, the remaining oscillations are located near to layers. Moreover, higher order approximations in time provide solutions with less oscillations.

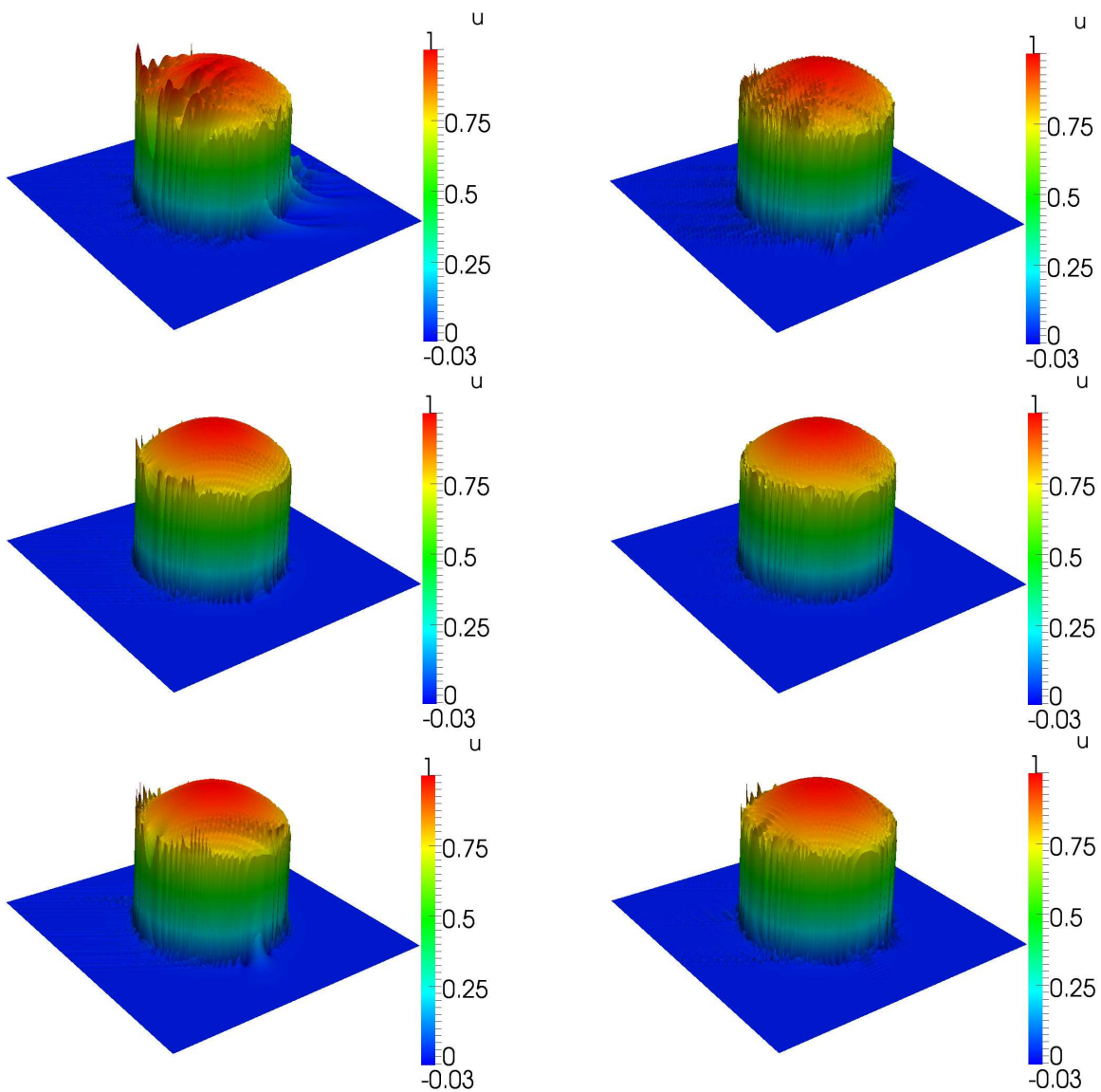


FIGURE 2. Example 3: numerical solution at $t = 0.5$, left: cGP(2) with $V_h = \mathbb{Q}_2^{\text{bubble}}$, $D(K) = \mathbb{P}_1(K)$, right: cGP(3) with $\mathbb{Q}_3^{\text{bubble}}$, $D(K) = \mathbb{P}_2(K)$; top to bottom: $\mu_0 = 0.01$, $\mu_0 = 0.1$, $\mu_0 = 1.0$.

REFERENCES

- [1] N. Ahmed and G. Matthies. Numerical study of SUPG and LPS methods combined with higher order variational time discretization schemes applied to time-dependent convection-diffusion-reaction equations. Preprint 1948, Weierstraß-Institut für Angewandte Analysis und Stochastik, Berlin, 2014.
- [2] N. Ahmed, G. Matthies, L. Tobiska, and H. Xie. Discontinuous galerkin time stepping with local projection stabilization for transient convection-diffusion-reaction problems. *Comput. Methods Appl. Mech. Engrg.*, 200:1747–1756, 2011.
- [3] A. K. Aziz and P. Monk. Continuous finite elements in space and time for the heat equation. *Math. Comp.*, 52(186):255–274, 1989.

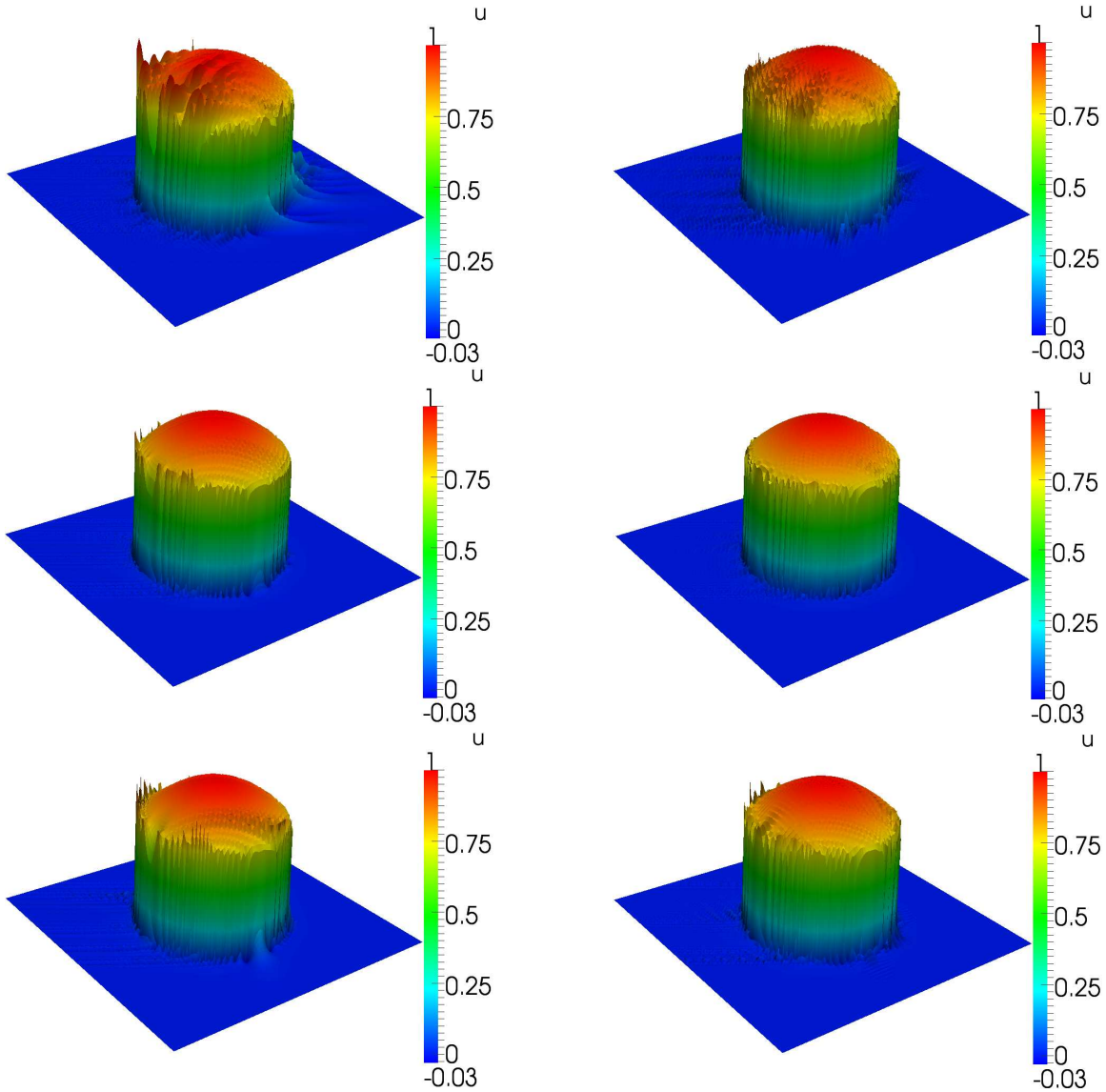


FIGURE 3. Example 3: numerical solution at $t = 0.5$, left: dG(2) with $V_h = \mathbb{Q}_2^{\text{bubble}}$, $D(K) = \mathbb{P}_1(K)$, right: dG(3) with $\mathbb{Q}_3^{\text{bubble}}$, $D(K) = \mathbb{P}_2(K)$; top to bottom: $\mu_0 = 0.01$, $\mu_0 = 0.1$, $\mu_0 = 1.0$.

- [4] R. Becker and M. Braack. A finite element pressure gradient stabilization for the Stokes equations based on local projections. *Calcolo*, 38(4):173–199, 2001.
- [5] R. Becker and M. Braack. A two-level stabilization scheme for the Navier-Stokes equations. In *Numerical mathematics and advanced applications*, pages 123–130. Springer, Berlin, 2004.
- [6] P. B. Bochev, M. D. Gunzburger, and J. N. Shadid. Stability of the SUPG finite element method for transient advection-diffusion problems. *Comput. Methods Appl. Mech. Engrg.*, 193(23-26):2301–2323, 2004.
- [7] M. Braack and E. Burman. Local projection stabilization for the Oseen problem and its interpretation as a variational multiscale method. *SIAM J. Numer. Anal.*, 43(6):2544–2566, 2006.
- [8] E. Burman. Consistent SUPG-method for transient transport problems: stability and convergence. *Comput. Methods Appl. Mech. Engrg.*, 199(17-20):1114–1123, 2010.

- [9] E. Burman and M. A. Fernández. Finite element methods with symmetric stabilization for the transient convection-diffusion-reaction equation. *Comput. Methods Appl. Mech. Engrg.*, 198(33-36):2508–2519, 2009.
- [10] P. G. Ciarlet. *The finite element method for elliptic problems*. North-Holland Publishing Co., Amsterdam, 1978. Studies in Mathematics and its Applications, Vol. 4.
- [11] R. Codina. Comparison of some finite element methods for solving the diffusion-convection-reaction equation. *Comput. Methods Appl. Mech. Engrg.*, 156(1-4):185–210, 1998.
- [12] K. Eriksson, D. Estep, P. Hansbo, and C. Johnson. *Computational differential equations*. Cambridge University Press, Cambridge, 1996.
- [13] K. Eriksson, C. Johnson, and V. Thomée. Time discretization of parabolic problems by the discontinuous Galerkin method. *RAIRO Modél. Math. Anal. Numér.*, 19(4):611–643, 1985.
- [14] M.-C. Hsu, Y. Bazilevs, V. M. Calo, T. E. Tezduyar, and T. J. R. Hughes. Improving stability of stabilized and multiscale formulations in flow simulations at small time steps. *Comput. Methods Appl. Mech. Engrg.*, 199(13-16):828–840, 2010.
- [15] T. J. R. Hughes and A. N. Brooks. A multidimensional upwind scheme with no crosswind diffusion. In *Finite element methods for convection dominated flows (Papers, Winter Ann. Meeting Amer. Soc. Mech. Engrs., New York, 1979)*, volume 34 of *AMD*, pages 19–35. Amer. Soc. Mech. Engrs. (ASME), New York, 1979.
- [16] S. Hussain, F. Schieweck, and S. Turek. Higher order Galerkin time discretizations and fast multigrid solvers for the heat equation. *J. Numer. Math.*, 19(1):41–61, 2011.
- [17] S. Hussain, F. Schieweck, and S. Turek. A note on accurate and efficient higher order Galerkin time stepping schemes for the nonstationary Stokes equations. *Open Numer. Methods J.*, 4:35–45, 2012.
- [18] V. John and P. Knobloch. On spurious oscillations at layers diminishing (SOLD) methods for convection-diffusion equations. I. A review. *Comput. Methods Appl. Mech. Engrg.*, 196(17-20):2197–2215, 2007.
- [19] V. John and P. Knobloch. On the performance of SOLD methods for convection-diffusion problems with interior layers. *Int. J. Comput. Sci. Math.*, 1(2-4):245–258, 2007.
- [20] V. John and P. Knobloch. On spurious oscillations at layers diminishing (SOLD) methods for convection-diffusion equations. II. Analysis for P_1 and Q_1 finite elements. *Comput. Methods Appl. Mech. Engrg.*, 197(21-24):1997–2014, 2008.
- [21] V. John and G. Matthies. MoonMD—a program package based on mapped finite element methods. *Comput. Vis. Sci.*, 6(2-3):163–169, 2004.
- [22] V. John and J. Novo. Error analysis of the SUPG finite element discretization of evolutionary convection-diffusion-reaction equations. *SIAM J. Numer. Anal.*, 49(3):1149–1176, 2011.
- [23] V. John and E. Schmeier. Finite element methods for time-dependent convection-diffusion-reaction equations with small diffusion. *Comput. Methods Appl. Mech. Engrg.*, 198(3-4):475–494, 2008.
- [24] P. Knobloch. On the application of local projection methods to convection-diffusion-reaction problems. In *BAIL 2008—boundary and interior layers*, volume 69 of *Lect. Notes Comput. Sci. Eng.*, pages 183–194. Springer, Berlin, 2009.
- [25] P. Knobloch. A generalization of the local projection stabilization for convection-diffusion-reaction equations. *SIAM J. Numer. Anal.*, 48(2):659–680, 2010.
- [26] G. Lube and D. Weiss. Stabilized finite element methods for singularly perturbed parabolic problems. *Appl. Numer. Math.*, 17(4):431–459, 1995.
- [27] G. Matthies and F. Schieweck. Higher order variational time discretizations for nonlinear systems of ordinary differential equations. Preprint 23/2011, Fakultät für Mathematik, Otto-von-Guericke-Universität Magdeburg, 2011.
- [28] G. Matthies, P. Skrzypacz, and L. Tobiska. A unified convergence analysis for local projection stabilisations applied to the Oseen problem. *M2AN Math. Model. Numer. Anal.*, 41(4):713–742, 2007.
- [29] G. Matthies, P. Skrzypacz, and L. Tobiska. Stabilization of local projection type applied to convection-diffusion problems with mixed boundary conditions. *Electron. Trans. Numer. Anal.*, 32:90–105, 2008.
- [30] W. H. Reed and T. R. Hill. Triangular mesh methods for the neutron transport equation. *Tech. Report LA-UR-73-479*, Los Alamos Scientific Laboratory, 1973.
- [31] H.-G. Roos, M. Stynes, and L. Tobiska. *Robust numerical methods for singularly perturbed differential equations. Convection-diffusion-reaction and flow problems*, volume 24 of *Springer Series in Computational Mathematics*. Springer-Verlag, Berlin, second edition, 2008.
- [32] F. Schieweck. A-stable discontinuous Galerkin-Petrov time discretization of higher order. *J. Numer. Math.*, 18(1):25–57, 2010.
- [33] D. Schötzau and C. Schwab. An hp a priori error analysis of the DG time-stepping method for initial value problems. *Calcolo*, 37(4):207–232, 2000.
- [34] D. Schötzau and C. Schwab. hp -discontinuous Galerkin time-stepping for parabolic problems. *C. R. Acad. Sci. Paris Sér. I Math.*, 333(12):1121–1126, 2001.
- [35] V. Thomée. *Galerkin finite element methods for parabolic problems*, volume 25 of *Springer Series in Computational Mathematics*. Springer-Verlag, Berlin, 1997.